GEOPHYSICS, VOL. 60, NO. 4 (JULY-AUGUST 1995); P. 998-1006, 6 FIGS., 2 TABLES.

The effect of steam quality on the electrical behavior of steam-flooded sands: A laboratory study

David B. Butler* and Rosemary J. Knight*

ABSTRACT

Laboratory measurements of the effects of steam injection on the electrical conductivity of sands can aid in the interpretation of electrical surveys used to monitor subsurface steam-injection projects. The effect of variations in injected steam quality was measured in the experiments presented here. The injection of low-quality steam, boiled from a 0.01 mol/L NaCl solution, into clean sand saturated with 0.01 mol/L NaCl, resulted in a net decrease in conductivity and a constant equilibrium conductivity in the steam zone, The injection of high-quality steam, using the same saturating and injection salinities, caused the conductivity to first drop to a minimum and then to increase to an equilibrium value similar to that seen in the low-quality injection. The local conductivity minimum deepened with time and traveled with the steam front. The appearance of the conductivity minimum at the steam front can be attributed to the formation of a dilution bank, which temporarily decreases the local salinity. The extent of the dilution increases with time, resulting in the decrease of the conductivity over time. The conductivity then increases as injected salt moves through the sand. The steam quality controls the appearance of this minimum because it determines the relative speeds of the steam front and the steam liquid: a minimum will not occur if the steam front moves more slowly than the steam liquid.

INTRODUCTION

Subsurface steam injection has been used for over 30 years in enhanced-oil-recovery operations (Doscher and Ghassemi, 1981). In recent years, steam injection has also proven to be an effective technique for removing certain types of nonaqueous-phase-liquid contaminants from the near-surface (Stewart and Udell, 1988). Its overall effectiveness as a recovery technique depends in part on how much of the subsurface is treated with steam. To ensure that all oil- or contaminant-bearing regions are treated, a reliable mapping technique is required. Monitoring wells provide accurate information at isolated positions but do not usually provide the density of coverage that is required.

Electrical surveys are capable of detecting steam-induced changes in conductivity, which is a function of temperature, salinity, and oil or contaminant saturation. A number of surveys have been successfully used to detect subsurface conductivity changes that occurred as a result of the injection of steam. These studies include surface measurements (Wayland et al., 1987), correlations of borehole-resistivity and temperature logs (Ranganayaki et al., 1990), and borehole-to-borehole tomography (Ramirez et al., 1993). Proper interpretation of the electrical data requires an understanding of the fluid processes occurring as a result of steam injection and of the associated variations in electrical conductivity.

Injected steam is generally a mixture of steam vapor (the gas phase of steam) and steam liquid (the liquid phase of steam); thus the steam zone, where the steam vapor exists, can contain steam liquid and original pore fluid. There is much interest in determining the conductivity changes likely to occur at the steam front, the downstream edge of the steam zone, as the detection of the front is most useful for monitoring purposes. Numerical models have been developed that describe the mass and heat transport during steam displacement of either water or water and oil (Menegus and Udell, 1985; Stewart and Udell, 1988; and Falta et al., 1992). These studies showed that an increase in temperature occurs in a narrow region ahead of the steam front, and that a decrease in water saturation occurs in a narrow zone immediately behind the steam front. An experimental and numerical study investigated the effects on conductivity caused by injecting steam boiled from distilled water into a salt-water-saturated sand pack (Vaughan et al., 1993). The study illustrated the impact on conductivity of the steam condensate that forms ahead of the steam front. The conductivity

Manuscript received by the Editor June 30, 1994; revised manuscript received November 18, 1994.
*Department of Geoph ysics and Astronomy, University of British Columbia, Vancouver, British Columbia, V6T 124 Canada.

measurements showed how the dilution of salt water by the steam condensate dominated the electrical response.

There is an additional factor that must be considered in many field applications where salt water, rather than fresh, is used as the feed water: this being the transport of salt in the steam liquid. The presence of saline liquid in the steam zone can have a significant effect on the electrical conductivity. For a given salinity of the steam liquid, the specific temporal and spatial conductivity changes seen in a steam zone are determined by the speed at which the steam liquid moves through the steam zone relative to the steam front. This relative speed is determined by the steam quality, defined as the fraction of the injected mass flux that is steam vapor. The experiments reported here show how steam quality, through this link to salt transport in the steam zone, affects the electrical conductivity both in, and ahead of, the steam zone.

PARAMETERS AFFECTING ELECTRICAL CONDUCTIVITY

The electrical conductivity of clean (clay-free) sands and sandstones can be described using Archie's equation (Archie, 1942)

$$\sigma_f = \phi^m S_w^n \sigma_w, \tag{1}$$

where σ_f is the formation conductivity, ϕ is porosity, S_w is the water saturation, σ_w is the conductivity of the pore fluid, and m and n are the cementation and saturation exponents. Archie (1942) found that m is approximately 1.8 to 2.0 for consolidated sandstones, and 1.3, the value used in this study, is an appropriate value for clean, unconsolidated sands. Steam injection can affect the electrical conductivity by changing the liquid water saturation in the reservoir, by changing the salinity of the pore fluid, and by increasing the temperature. Secondary influences include steam-induced changes in fluid pressure and matrix wettability.

The water saturation will vary during a steam flood as a result of the displacement by steam of water, oil, or contaminant. Original S_w levels in a reservoir can vary widely, as can water saturations in a steamed region. Minimum water saturations in a steam zone, however, are not likely to be less than 0.10 to 0.15. This level is supported both by theoretical considerations (Menegus and Udell, 1985), and field estimates (Mansure and Meldau, 1990). Menegus and Udell (1985) found that the equilibrium steam-zone water saturation depends in part upon the geometry of the injection process, with the minimum saturation obtained when steam is injected into the top of a formation and forces fluids downwards. The effect of water-saturation variations is included explicitly in Archie's law in the term S_w^n. The saturation exponent n, over saturations ranging from 0.15 to 1.0, was determined by Archie (1942) to be approximately 2.0, the value used in this study.

Potentially, large salinity contrasts can be caused by the injection of steam. Oil-reservoir salinities can be as high as 3.1 mol/L (Worthington et al., 1990). The extent to which salinity is reduced depends on the salinity and speed of the steam liquid and on the rate of condensation at the steam front. The increase in conductivity with salinity is approximately linear for low salinities but becomes substantially nonlinear at higher salinities. A number of researchers have published theoretically-based formulas relating conductivity to salinity (Ellis, 1987; Robinson and Stokes, 1965). The most widely applicable formulas for calculating the conductivity of NaCl solutions are empirical relations given in Worthington et al. (1990) for the salinity ranges 10^{-4} M to 0.1 M, 0.09 M to 1.4 M, and 1.0 M to 5.35 M. The equation for the dilute range, used in this study, is

$$\begin{aligned}\log \sigma_w = {} & 0.942203 + 0.8889000 \log c \\ & - 2.72398 * 10^{-2} (\log c)^2 \\ & - 2.25682 * 10^{-3} (\log c)^3 \\ & + 1.46605 * (\log c)^4,\end{aligned} \tag{2}$$

where σ_w is in S/m, and c is the ionic concentration in mol/L. Equation (2) was shown to predict measured data to within 0.1%.

The injection of steam will clearly cause an increase in reservoir temperature. Theoretical studies reported by Stewart and Udell(1988) showed that steam injection produced a narrow heated zone ahead of the steam front. Therefore the effects of increased temperature are restricted to regions within or very close to the steam zone. Increasing the temperature of a clean sand increases its electrical conductivity, mainly because of changes in the conductivity of the pore water. Steam injection in oil reservoirs is unlikely to cause temperatures to exceed 300°C (Mansure and Meldau, 1990). Temperature corrections are most commonly made using Arps's law (Arps, 1953)

$$\frac{\sigma_2}{\sigma_1} = \frac{(T_2 + 21.5)}{(T_1 + 21.5)}, \tag{3}$$

where T is in degrees Celsius. This is a least-squares linear fit to the conductivity of NaCl solutions at temperatures between 0 and 156 degrees Celsius. It tends to overestimate the conductivity of more concentrated solutions at elevated temperatures (Sen and Goode, 1992). Other corrections are given by Heiland (1940); Llera et al. (1990); Sen and Goode (1992); and Vaughan et al, (1993).

The steam quality has long been assumed to play a role in the development of the subsurface electrical conductivity, but its full effect is unknown. Menegus and Udell (1985) show how varying the steam quality can affect the steam-zone water saturation. Given the potentially large salinity-induced variations in conductivity, any link between steam quality and salinity would constitute an important mechanism that must be considered when interpreting electrical data. The laboratory apparatus discussed below was developed to determine how steam quality affects the conductivity of steam-flooded sands.

EXPERIMENTAL APPARATUS AND PROCEDURE

The steam injection apparatus is shown in Figure 1. The electrical conductivity cell consists of a 32.5-cm long, 13.9-cm diameter ceramic tube, sealed at both ends with stainless-steel plates and filled with Ottawa sand. The sand is comprised of greater than 99% quartz; the grains are spherical to subspherical and are well rounded. Steam is injected at the top plate, heating the system, and forcing fluid out the bottom of the vessel. Eleven thermocouples, inserted through the ceramic wall, measure temperature every 2.5 cm along the axis of the cell. Heating coils and thermocouples

attached to the outside of the cell are used to set the external temperature distribution equal to the internal distribution, to minimize heat losses and to promote 1-D fluid and current flow. Electrical conductivity is measured using a four-electrode technique: the steel plates act as the current electrodes, and the thermocouple sheaths act as the potential electrodes. A computer measures and records the conductivity and temperature distributions every 2.5 s.

This cell is a modification of a design described by Vaughan et al. (1993) that used a 5.08-cm diameter, approximately 75-cm long, horizontal glass tube. Vaughan et al. (1993) reported that a steam override likely occurred in the experiments because of the cell's horizontal orientation. In the experiments reported here, the conductivity cell was oriented vertically to better promote the stable advance of a 1-D steam front. The dimensions of the cell were also changed to improve the resistive measurement limit of the cell.

Electrical conductivity is measured by passing a 10-V square wave across a series arrangement of a precision resistor and the sand pack. The alternating current is necessary for the removal of electrochemical voltages set up between the thermocouples and the endplates. A frequency of 100 Hz is used since few capacitive effects are produced, and the sampling rate is fast enough to capture all conductivity changes. The current passing through the sand is determined by the voltage across the precision resistor. Assuming 1-D current flow, the conductivity of the sand between successive thermocouples is

$$\sigma = \frac{LV_p}{AR_pV}, \tag{4}$$

where L is the distance between a neighboring pair of thermocouples, V_p is the voltage across the precision resistance R_p, A is the cell cross-sectional area, and V is the voltage measured between thermocouples.

An important aspect of the system is the steam generator, which was constructed by wrapping the 3.2-mm, stainless-steel fluid tubing around a cartridge heater, insulating the tubing, and pressing it into a dewar flask. Since it is a one-pass boiler, whatever fluids are pumped into the boiler are then injected into the cell. Any salt in the feed water remains in the steam liquid. By adjusting the heater's input electrical power, the steam quality can be set to any desired value between zero and one. Volumetric flow rates into the boiler are kept constant throughout an experiment. The mass flux leaving the boiler and entering the sand is equivalent to that entering the boiler from the pump. The steam quality therefore determines the steam-vapor and steam-liquid mass-injection rates.

A typical experiment starts with the evacuation of the measurement cell. The sand is then saturated and flushed with three pore volumes of the initial solution. The pump and fluid lines are then flushed with the displacing fluid. When the pump and heaters are started, flow is diverted past the measurement cell until the heating system has reached an equilibrium temperature. Monitoring of the temperatures and conductivities is then started, and ten minutes later, the steam is diverted into the sand. The steam injection continues until steam nears the downstream end of the cell, at which point the heaters are turned off, cold water is injected, and the conductivity monitoring stops. One experiment takes up to three hours.

RESULTS

A series of experiments were conducted to determine the effects of feedwater salinity and steam quality on the electrical conductivity of unconsolidated sand. A displacement

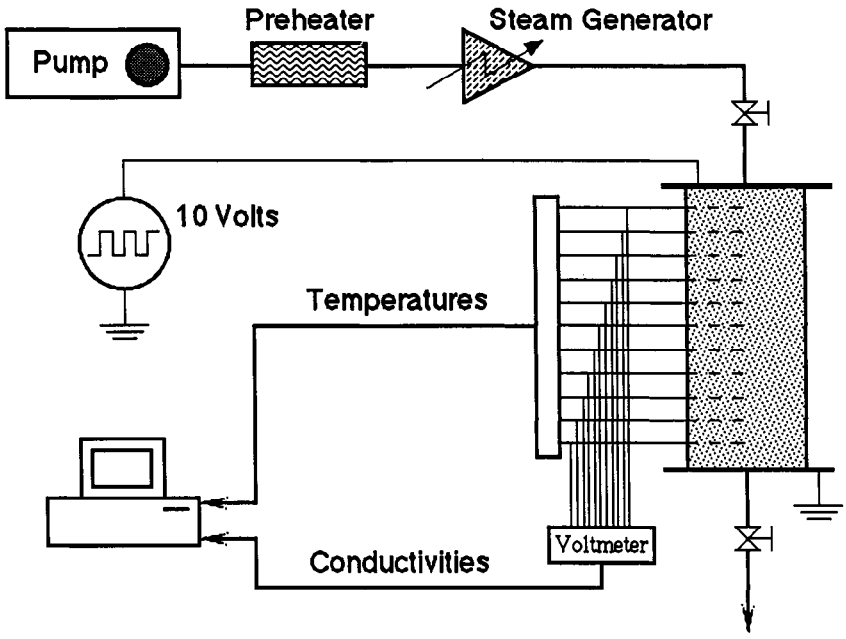

FIG. 1. Laboratory apparatus used to measure electrical conductivity during steam injection.

of salt-water-saturated sand with low-quality steam, boiled from distilled feedwaters, served as a test of the cell, and as a baseline for further experiments. The second experiment was a repeat of the first, except that saline feedwaters were used. The third experiment was a repeat of the second, except that high-quality steam was used. Parameters describing the experiments are summarized in Table 1. All experiments used identical initial pore-fluid salinities and identical volumetric flow rates into the boiler. The flow rate was chosen because it was found to produce a stable, l-D, steam-front advance. Volumetric flow rates into the sand increased in the third experiment because of the higher steam quality.

In the first experiment, the sand was initially saturated with 0.01 M NaCl and flushed with 17%-quality steam. The boiler feedwaters were distilled, and so the resulting two-phase mixture consisted of steam vapor and distilled steam liquid. The results are shown in Figure 2.

Temperatures are point measurements made at the 11 thermocouples along the cell's axis. Temperature at each thermocouple began at approximately 20°C then increased with the approach of the steam front. Arrival of the steam front at a thermocouple is marked by the point where the temperature becomes constant, near 100°C.

Conductivity is averaged over the regions between neighboring thermocouples; thus there are ten conductivity traces in Figure 2, showing the changes in conductivity in ten regions as a function of time. The sand initially had a uniform conductivity of 0.022 S/m, which can be seen in Figure 2 as the starting point for all conductivity traces. Conductivity in the uppermost region of the sand (corresponding to conductivity trace σ_1 at the left of Figure 2) increased slightly soon after injection began, but then fell rapidly by more than two orders of magnitude. Deeper regions in the sand displayed similar behavior. Some traces showed a temporary conductivity increase before the arrival of the steam front, followed by a decrease as the steam front passed through the region. After steam swept through the sand, conductivities approached equilibrium values below 10^{-4} S/m.

Table 1. Experimental parameters for the three steam injections: q is the volumetric flow rate into the boiler, C_0 is the salinity of the boiler feedwaters, and C_{sat} is the initial pore-fluid salinity.

#	q (ml/min)	C_0 (mol/L)	C_{sat} (mol/L)	Quality
1	15.9	distilled	0.01	0.17 ± 0.02
2	15.9	0.01	0.01	0.17 ± 0.02
3	15.9	0.01	0.01	0.62 ± 0.02

The second experiment injected 17%-quality steam boiled from 0.01 M NaCl, identical to the saturating fluid. The conductivity and temperature results for this experiment are shown in Figure 3. The temperature response at all positions in the cell was identical to that seen in the first experiment. Conductivity in the uppermost region first increased by a factor of two, dropped as the steam approached, and then reached an equilibrium value of 0.04 S/m, significantly more conductive than in the first experiment. The other regions behaved similarly, except that the initial increase was gradually reduced over the length of the cell, reaching a factor of 1.4 at the downstream end. All regions reached a stable steam-zone conductivity of 0.04 S/m. None of the traces displayed the temporary conductivity peaks seen in the first experiment just prior to the arrival of the steam front.

The third experiment was a repeat of the second, except that the injected steam quality was increased to 62%. Results are shown in Figure 4. The steam penetrated much more quickly into the sand, reducing the time required for the steam front to reach the end of the cell by half. Temperature did not increase in the sand until just before the arrival of the steam front. Conductivities in the upper three regions of the sand again increased as the temperature increased, although the magnitude of the increases was less than the previous experiment, and increases were not seen in regions farther into the sand. All of the regions showed conductivities in the steam zone that varied with time. With the approach of the steam front, conductivity dropped to a minimum, then

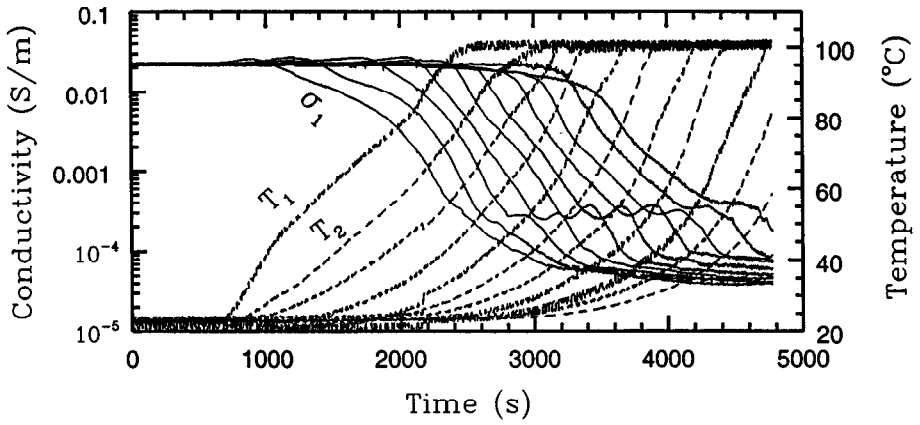

FIG. 2. Conductivity and temperature distributions from ex eriment #l. The sand was initially saturated with 0.01 M NaCl and was flushed with 17%-quality steam boiled from distilled water. The eleven dashed lines indicate temperatures at each thermocouple tip measured along the axis of the cell. The ten solid lines represent the average conductivities between successive pairs of the eleven thermocouple sheaths. For example, thermocouples T_1 and T_2 are located 2.5 cm and 5.1 cm, respectively, from the top of the cell; trace σ_1 represents the average conductivity between thermocouples T_1 and T_2.

started to increase again towards an equilibrium value. The minimum deepened as it traveled, so that the region near the steam front became progressively less conductive as the front moved through the sand. After 1500 s, the conductivity of a given measurement zone reached a minimum when the steam front reached the downstream edge of the zone.

DISCUSSION

The first experiment, which used distilled boiler feedwaters, was conducted to test the ability of the apparatus to detect steam-induced changes in conductivity and was intended to act as a baseline against which other results could be compared. The sand-pack porosity, injection mass flux, and initial pore-fluid salinity were similar to those used in run 106 of Vaughan et al. (1993), while the steam quality was lower (17% versus 48%). The conductivity profiles from this experiment qualitatively match their results.

The electrical response of the sand in the first experiment can be explained as the result of changes in temperature, salinity, and water saturation. Referring to Figure 2, temperatures at the first and second thermocouples (T_1 and T_2) started to increase at 700 and 800 s. The steam front arrived at these two locations at 2500 and 3100 s. The average conductivity between these two thermocouples (σ_1) increased from 700 to 900 s, because of the increased temperature, but then rapidly decreased. The decrease, caused by the arrival of distilled water that dramatically reduced the local salinity continued until the steam front reached the first thermocouple. In the period from 2500 to 3100 s, σ_1 decreased because of the continued salinity reduction and the displacement of liquid water by resistive steam vapor. Once the steam front passed the measurement location, the water saturation, temperature, and salinity all reached stable values, resulting in a stable electrical conductivity. This general behavior can be used to explain most features of the conductivity responses from deeper in the sand. However, the continued movement of distilled water ahead of the steam front moved the region of rapid salinity decrease farther ahead of the steam front, and the salinity close to the steam front became more homogeneous. Thus, after 2500 s, initial temperature-related conductivity increases were not seen, as salinity effects dominated. After 3100 s, conductivity temporarily increased immediately prior to the steam-front arrival because temperature effects now dominate in this

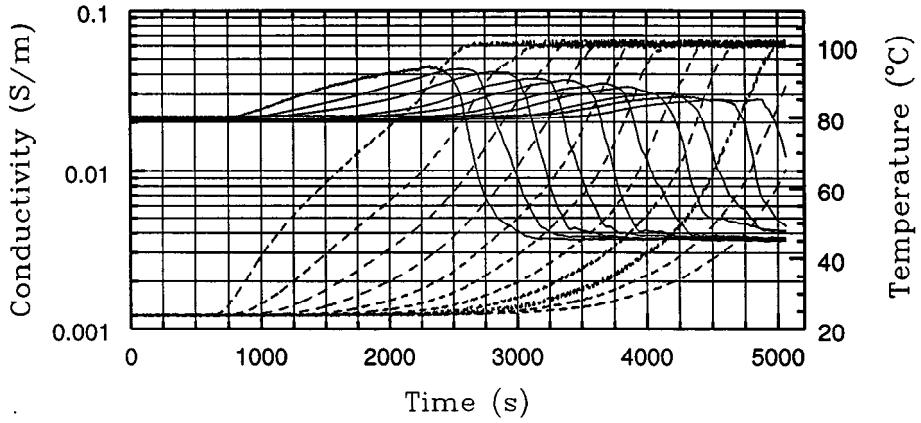

FIG. 3. Conductivity and temperature distributions from experiment #2. The sand was initially saturated with 0.01 M NaCl and was flushed with 17%-quality steam boiled from 0.01 M NaCl.

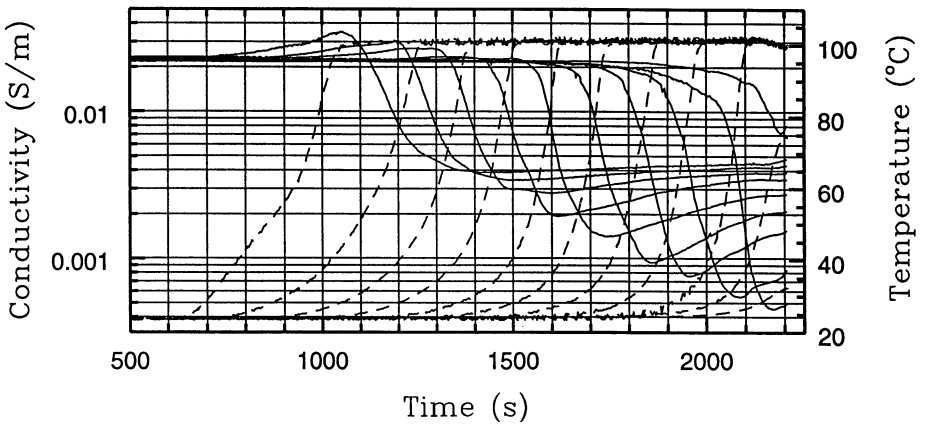

FIG. 4. Conductivity and temperature distributions from experiment #3. The sand was initially saturated with 0.01 M NaCl and was flushed with 62%-quality steam boiled from 0.01 M NaCl.

region. Conductivity then began to decrease again as resistive steam vapor displaces liquid water. This injection scenario was thoroughly discussed and modeled in Vaughan et al. (1993). The reproduction of their results is viewed as a validation of the experimental set-up.

Figure 3 shows how the use of slightly saline boiler feedwaters affects the conductivity: the initial temperature-related conductivity increase was greatly enhanced, and conductivity in the steam zone was 100 times greater than that seen when distilled feedwaters were used. The enhancement of the temperature effect implied a reduced dilution of salinity ahead of the steam front: salt traveling in the steam liquid kept up with the steam front and remixed with the distilled steam condensate. Some dilution still occurred, as evidenced by the reduction over time of the temperature effect and the drop in conductivity in each region before the arrival of the steam front. Again, once the steam front passed by a measurement region, the region's conductivity became constant over time, implying constant temperature, water-saturation, and salinity conditions.

A comparison of Figures 3 and 4 shows how steam quality can affect the conductivity in and near the steam zone. The low-quality injection results in an equivalent conductivity everywhere in the steam zone, and this conductivity remains constant over time. In the high-quality injection, the conductivity in the steam zone changes over time, first reaching a minimum, then increasing to an equilibrium value. This equilibrium value, at later times, appears to be equivalent everywhere in the steam zone. The high quality behavior can be explained first by a progressive dilution of the salinity at the steam front because of the condensation of steam vapor, and second, by a later salinity increase as the saline steam liquid moves through the sand. Increasing the steam quality has two effects: it increases the heat delivered to the front, thereby increasing its speed, and it decreases the amount of steam liquid in the injected fluid, thereby decreasing the steam-liquid speed. The appearance of the conductivity minimum depends on the relative speeds of the steam front and the steam liquid. If the steam front moves more quickly, then a minimum will appear. If instead the speed of the steam liquid exceeds that of the steam front, no minimum will appear because the injected salt will keep up with the steam front and mask the dilution effects of the distilled condensate. For the experimental results shown here, the steam liquid was estimated to have moved more quickly than the steam front in the second experiment but more slowly than the steam front in the third.

Numerical modeling of high-steam-quality results

The high-steam-quality results suggest that a unique and easily identifiable electrical signature, caused by the development of a distilled condensate bank, can be associated with the steam front. To test the validity of this concept, the electrical response of a high-steam-quality injection was numerically modeled. The response can be modeled, as shown in Figure 5, by treating the process as the sum of two simple systems-a water-zone system and a steam-zone system. The water-zone system models the transport of heat and solute ahead of the steam front. The steam-zone system models the transport of solute in the steam liquid, as well as the progressive dilution of original pore fluid at the steam front. Temperature, salt-concentration, and water-saturation profiles are calculated separately for both zones, the solutions combined, and the conductivity profile calculated.

The water zone is considered in a moving reference frame that is attached to the steam front, traveling at the steam front velocity v_f. Both the salt transport and heat transport in this reference frame are described by advective-dispersive equations:

$$D\frac{\partial^2 c}{\partial u^2} - v_{ww}\frac{\partial c}{\partial u} = \frac{\partial c}{\partial t}, \tag{5}$$

$$\alpha\frac{\partial^2 T}{\partial u^2} - \beta\frac{\partial T}{\partial u} = \frac{\partial T}{\partial t}, \tag{6}$$

where u is the distance ahead of the steam front, c is the salt concentration, T is the temperature, and D is the ionic dispersion coefficient. V_{ww} is the pore-water velocity relative to the steam front

$$V_{ww} = \frac{q}{A\phi} - v_f S'_w, \tag{7}$$

where q is the volumetric pump rate, and S'_w is the steam-zone equilibrium water saturation. The terms α and β are defined as

$$\alpha = k_T\phi/[\rho\phi C_p + (1-\phi)\rho_s C_s], \tag{8}$$

$$\beta = v_{ww}\rho C_p\phi/[\rho\phi C_p + (1-\phi)\rho_s C_s], \tag{9}$$

where k_T is the thermal conductivity of the water-saturated sand, ρ is the density of the water, ρ_s is the density of the sand grains, C_p is the heat capacity of the water, and C_s is the sand-grain heat capacity. The initial salinity C_{init} is set to C_{sat}, the original pore-fluid salinity, and the boundary conditions are

$$c(0,t) - \frac{D}{V_{ww}}\frac{\partial c(u,t)}{\partial u}\Big|_{u=0+} = C_{inj}, \tag{10}$$

$$c(\infty,t) = C_{init}, \tag{11}$$

where C_{inj}, the salinity of water injected at the steam front, is set to a value that represents the conductivity of condensate, i.e., distilled water. The corresponding solution is given by Kreft and Zuber (1978)

$$\frac{c(u,t)-C_{init}}{C_{inj}-C_{init}} = \frac{1}{2}erfc\left(\frac{u-v_{ww}t}{2\sqrt{Dt}}\right) - \frac{1}{2}\exp\left(\frac{v_{ww}u}{D}\right)erfc\left(\frac{u+v_{ww}t}{2\sqrt{Dt}}\right)\times\left[1+\frac{v_{ww}(u+v_{ww}t)}{D}\right] + \frac{v_{ww}t}{\sqrt{\pi Dt}}\exp\left(\frac{(u-v_{ww}t)^2}{4Dt}\right). \tag{12}$$

The initial temperature T_{init} is set to room temperature.

Thermal boundary conditions are

$$T(0, t) = T_{inj}, \tag{13}$$

$$T(\infty, t) = T_{init}, \tag{14}$$

where T_{inj} is set at the boiling temperature. The solution is (Ogata and Banks, 1961)

$$\frac{T(u, t) - T_{init}}{T_{inj} - T_{init}} = \frac{1}{2} erfc\left(\frac{u - \beta t}{2\sqrt{\alpha t}}\right) + \frac{1}{2} \exp\left(\frac{\beta u}{\alpha}\right) erfc\left(\frac{u + \beta t}{2\sqrt{\alpha t}}\right). \tag{15}$$

Thus the water-zone salinity and temperature distributions can be calculated analytically.

In the steam-zone model, temperature is fixed at that of the injected steam. The equilibrium water saturation is determined by assuming that the difference between cumulative water outflow and inflow is a result of the presence of steam vapor. The saturation distribution close to the steam front 'is then estimated using the method of Menegus and Udell (1985). An approximation to the salt-concentration profile can be obtained by splitting the steam zone into two parts, as shown in Figure 5b. One part looks downstream from the injection port and models salt transport in the steam liquid. The other part looks upstream from the steam front and models salt transport in the original pore fluid, which has been progressively diluted by steam condensate and left behind in the steam zone.

Looking downstream from the injection port, the steam zone is treated in a fixed reference frame, and the initial pore-fluid salinity throughout the zone is set to zero. The injection salinity is set to $C_0/(1 - f)$, where f is the steam quality, and C_0 is the boiler-feedwater salinity. The steam-liquid speed is set as $v_1 = q(1 - f)/(A\phi S'_w)$. Salt transport in this situation has an analytical solution of the form of equation (12).

Looking upstream from the steam front, the problem is again treated using a moving reference frame attached to the steam front. The initial concentration is set to C_{sat}, and the pore-water velocity v_2, directed backwards from the front towards the injection port, is the difference between the steam-front speed and v_1. The salinity boundary condition at the front, at any time, is set equal to the solution of

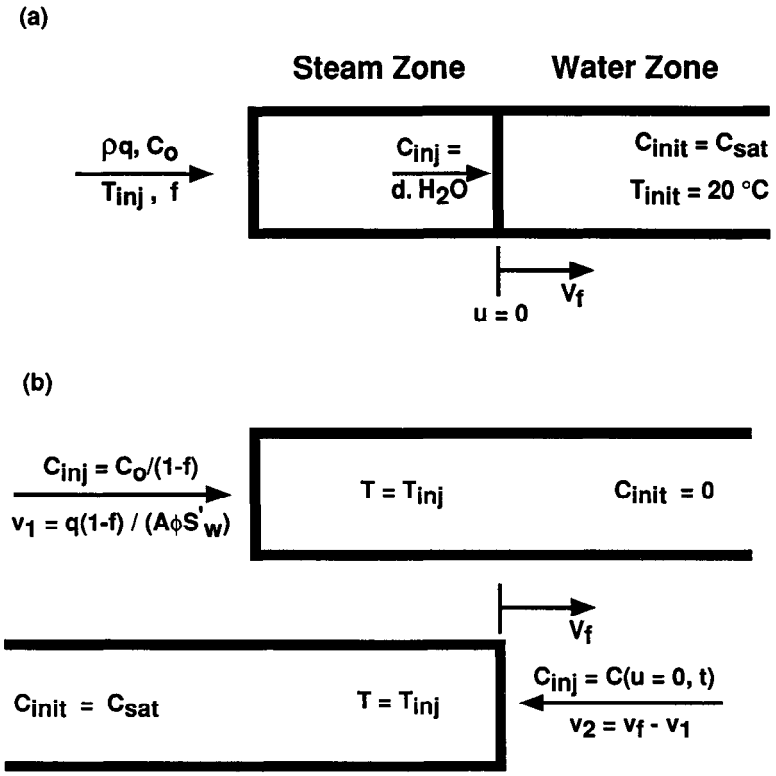

FIG. 5. A simplified approach to modeling the electrical conductivity response seen in the laboratory experiments. (a) Solutions for water-saturation, temperature, and salt-concentration profiles are calculated separately for both the steam zone and the water zone. The input parameters for the modeling include the steam-front speed v ; the total mass injection rate, which is the product of the room-temperature density of water ρ and the volumetric pump rate q; the salinities of the initial saturating fluid C_{sat} and the steam generator feedwaters C_0; the initial temperature T_{init}; the injected steam temperature T_{inj}; and, f, the steam quality. The salinity of distilled water (d. H_20) is an equivalent NaCl salinity that has the same electrical conductivity as distilled water. (b) The steam zone is split into two parts to model the transport of salt both in the steam liquid and in the original pore fluid left behind in the steam zone.

equation (12) at $u = 0$. Because of the time-varying boundary concentration, this problem does not have an analytical solution and is solved using a 1-D finite-difference calculation. The salinity in the steam zone is, to a first approximation, the sum of the upstream and downstream solutions over the region between the injection port and the steam front.

The water- and steam-zone solutions are then combined to obtain profiles of salinity, temperature, and water saturation as functions of time and distance along the cell. These profiles are then used with equations 1, 2, and 3 and the geometry of the cell electrodes to produce predicted conductivity curves.

Table 2 shows the values used for the numerical modeling of the third experiment. The arrival times of the steam front were chosen at each thermocouple as the point where the temperature became constant with time. A least-squares fit of the arrival-times-versus-distance was used to obtain the front velocity. The theoretical results are compared to the data in Figure 6. Modeled curves have been offset to the right by 250 s to account for an initial period during which the steam heated the top plate of the cell before advancing into the sand. The results show good agreement with the laboratory data: the modeled conductivity reaches a minimum and then climbs up to a stable equilibrium value. The match is not as good at the top of the cell, but this is to be expected since the flow regime close to the inlet is unlikely to be 1-D.

Table 2. Input parameters used in the numerical simulation of the third experiment.

A	0.0152 m^2
ϕ	0.33
k_T	4.0 W/m/K
ρ	998 kg/m^3
ρ_s	2650 kg/m^3
C_p	4220 J/kg/K
C_s	2000 J/kg/K
D	2.7×10^{-7} m^2/s
q	15.9 ml/min
f	0.65
v_f	2.0×10^{-4} m/s
S_w (steam zone; minimum)	0.14
C_{inj} (water zone)	6.0×10^{-5} mol/L NaCl
C_{sat}	0.01 mol/L NaCl
C_0	0.01 mol/L NaCl

The modeling approach is a simplified representation of the steam-injection process. Its chief limitation is that it does not allow for heat losses that affect the propagation of the steam front. The steam-front speed is calculated as an average over the whole experiment and does not account for the relatively slow progress of the front at the beginning of the experiment. Therefore the model overemphasizes the separation of distilled condensate and saline steam liquid in the early part of the injection, thereby underestimating the conductivity. This error cannot be completely corrected by shifting the modeled results in time. The technique of splitting the ion transport in the steam zone into two parts also leads to ionic dispersion errors, since the calculation in one direction is unaware of ions present because of the calculation in the other direction. This results in an overestimation of the steam-zone ionic gradients and a resulting overestimation of ionic dispersion effects. Neverthe-

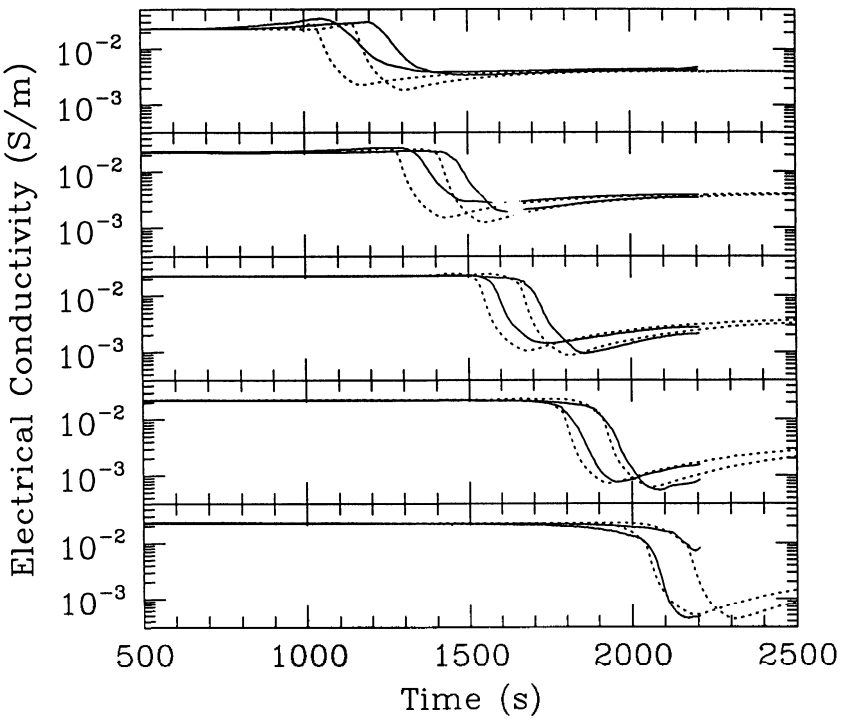

FIG. 6. A comparison of the data from the third experiment and the corresponding model results. Solid lines two sets of experimental data and model predictions, with the upper window corresponding to the upper two regions in the sand.

less, it is a useful technique for explaining observed laboratory results.

Steam injection in these experiments resulted in a net decrease in conductivity, in contrast to the increased conductivities seen in field experiments (Ranganayaki et al., 1990; Ramirez et al., 1993). The differences can be attributed to the effects of clay and nonconducting fluids such as oil. Clay is known to both increase the effects of temperature and to decrease the effects of changes in water saturation (Waxman and Thomas, 1974), thereby increasing the conductivity of a steam zone. Steam will also preferentially penetrate the most permeable parts of a reservoir, leaving clay lenses with high water saturations and correspondingly high conductivities. Oil reservoirs may also have smaller net changes in water saturation since steam displaces both oil and water instead of just water. Therefore the effects of steam saturation can be overemphasized in oil-free laboratory displacements.

SUMMARY AND CONCLUSIONS

The results of this laboratory study have shown that the electrical response of steam-flooded sands is significantly affected by the steam quality: a high-steam-quality injection can cause a dilution bank to form ahead of the steam front, resulting in a distinctive electrical behavior. The bank will form whenever the steam front moves more quickly than the steam liquid. This condition will be satisfied by high-steam-quality injections but not by low-quality injections. The bank will move with the steam front and can dominate the development of the steam-zone electrical conductivity, even when there is no bulk difference in salinity between the injected fluid and the initial pore fluid. The conductivity minimum deepens with distance and time as a result of the increasing dilution over time of the pore fluid ahead of the front. The salinity at a given position reaches a minimum as the steam front passes that position since the condensation and resulting dilution cease once the front passes by. The salinity at that position then immediately begins to increase as the more saline upstream water flows past. The conductivity at the steam front will continue to drop until the local salinity equals that of the condensing steam. At this point, the minimum will begin to broaden as the distance between the steam front and the steam liquid increases. The observed dependence on steam quality suggests that injection parameters could be selected to optimize the electrical signature associated with the steam front. For example, the conductivity minimum seen at the steam front in this study with high-quality steam would be easier to detect than a steadily decreasing conductivity.

The experiments reported here were conducted on clean, water-saturated sands. While working with this simple system has given us a good understanding of the electrical response of the steam zone, there is clearly a need to extend these studies to consider other parameters, such as another fluid and the presence of clays.

ACKNOWLEDGMENTS

The development and construction of the laboratory steamflood apparatus was funded by Mobil Exploration and Production Services and Mobil Research and Development. We are most grateful to Bill Troyer for initially suggesting this project, and to Jim Bulau and Ranga Ranganayaki for helpful discussions during the early stages of this research. Additional funding was obtained through an NSERC operating grant to Rosemary Knight. David Butler was supported by an NSERC scholarship, and by a Tri-Council Eco-Research scholarship. We wish to thank Ray Rodwell for his expert machining. We also thank Michael Wilt for his very helpful review of the paper.

REFERENCES

Archie, G. E., 1942, The electrical resistivity log as an aid in determining some reservoir characteristics: A.I.M.E., 146,54-67.
Arps, J. J., 1953, The effect of temperature on the density and electrical resistivity of sodium chloride solutions: Trans., A.I.M.E., 198, 327-330.
Doscher, T. M., and Ghassemi, F., 1981, Steam drive-the successful enhanced oil recovery technology, in Fayers, F. J., Ed., Enhanced oil recovery: Developments in Petroleum Science, 13, Elsevier Science Publ. Co., Inc., 549-562.
Ellis, D. V., 1987, Well logging for earth scientists: Elsevier Science Publ. Co., Inc.
Falta, R. W., Pruess, K., Javandel, I., and Witherspoon, P. A., 1992, Numerical modeling of steam injection for the removal of nonaqueous phase liquids from the subsurface 1. Numerical formulation: Water Resource Res., 28, 433-449.
Heiland, C. A., 1940, Exploration geophysics: Prentice-Hall, Inc.
Kreft, A., and Zuber, A., 1978, On the physical meaning of the dispersion equation and its solutions for different initial and boundary conditions: Chem. Eng. Sci., 33, 1471-1480.
Llera, F. J., Sato, M., Nakatsuka, K., and Yokoyama, H., 1990, Temperature dependence of the electrical resistivity of water saturated rocks: Geophysics, 55, 576-585.
Mansure, A. J., and Meldau, R. F., 1990, Steam-zone electrical characteristics for geodiagnostic evaluation of steam-flood performance: Soc. Petr. Eng. Formation Evaluation, 241-247.
Menegus, D. K., and Udell, K. S., 1985, A study of steam injection into water saturated capillary porous media, in Yao, L. S., Chen, M. M., Hickox, C. E., Simpkins, P. G., Chow, L. C., Kaviany, M., Cheng, P., and Davis, L. R., Eds., Heat transfer in orous media and particulate flows: Am. Soc. Mech. Eng., 46,151-157.
Ogata, A., and Banks, R. B., 1961, A solution of the differential equation of longitudinal dispersion in porous media: U.S. Geol. Surv. Prof. Pa er, 411-A.
Ramirez, A., Daily, W., LaBrecque, D., Gwen, E., and Chestnut, D., 1993, Monitoring an underground steam injection process using electrical resistance tomography: Water Resour. Res., 29, 7388.
Ranganayaki, R. P., Akturk, S. E., and Fryer, S. M., 1990, Formation resistivity variation due to steam flooding: A log study: Geophysics, 57, 488-494.
Robinson, R. A., and Stokes, R. H., 1965, Electrolyte solutions: Butterworth and Co., Ltd.
Sen, P. N., and Goode, P. A., 1992, Influence of temperature on electrical conductivity of shaly sands: G e ophysics, 57, 89-96.
Stewart, L. D., and Udell, K. S., 1988, Mechanisms of residual oil displacement by steam injection: Soc. Petr. Eng. Res. Eng., 3, 1233-1242.
Vaughan, P. J., Udell, K. S., and Wilt, M. J., 1993, The effects of steam injection on the electrical conductivity of an unconsolidated sand saturated with a salt solution: J. Geophys. Res., 98, No. Bl, 509-518.
Waxman, M. H., and Thomas, E. C., 1974, Electrical conductivities in shaly sands-1. The relation between hydrocarbon saturation and resistivity index; II. The tern erature coefficient of electrical conductivity: J. Petr. Tech., 26, 213-225.
Wayland, J. R., Jr., Lee, D. O., and Cole, T. J., 1987, CSAMT mapping of a Utah tarsand steamflood: Trans., A.I.M.E., 283,345-352.
Worthington, A. E., Hedges, J. H., and Pallatt, N., 1990, SCA guidelines for sample prep aration and porosity measurement of electrical resistivity samples: The Log Analyst, 31, 20-28.